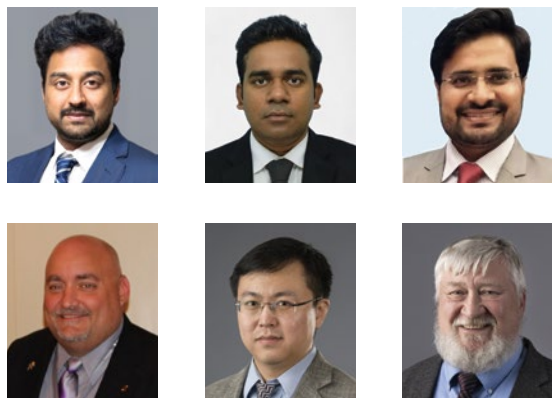


# Enhanced Bottom Anode Monitoring in DC Electric Arc Furnaces Using Fiber-Optic Sensors



## Authors

**Yeshwanth Reddy Mekala** (top left), Ph.D. Student, Department of Materials Science and Engineering, Missouri University of Science and Technology, Rolla, Mo., USA  
ymekala@mst.edu

**Ogbale C. Inalegwu**, Department of Electrical and Computer Engineering, Missouri University of Science and Technology, Rolla, Mo., USA

**Rony Kumer Saha** (top center), Department of Electrical and Computer Engineering, Missouri University of Science and Technology, Rolla, Mo., USA  
rsrt4@mst.edu

**Farhan Mumtaz** (top right), Assistant Research Professor, Department of Electrical and Computer Engineering, Missouri University of Science and Technology, Rolla, Mo., USA

**Rex E. Gerald II**, Department of Electrical and Computer Engineering, Missouri University of Science and Technology, Rolla, Mo., USA

**Jeffrey D. Smith** (bottom left), Research Associate Professor, Department of Materials Science and Engineering, Missouri University of Science and Technology, Rolla, Mo., USA  
jsmith@mst.edu

**Jie Huang** (bottom center), Department of Electrical and Computer Engineering, Missouri University of Science and Technology, Rolla, Mo., USA

**Ronald J. O'Malley** (bottom right), F. Kenneth Iverson Chair Professor for Steelmaking Technologies and Director, Kent D. Peaslee Steel Manufacturing Research Center, Missouri University of Science and Technology, Rolla, Mo., USA  
omalleyr@mst.edu

A pin-style bottom anode employs conductive steel rods that serve as the pathway for the high electrical power through rammed refractory at the bottom of a DC electric arc furnace (EAF). Anode wear during operation is important to monitor, as anode replacement is expensive and impacts EAF productivity. Liquid steel penetration into the unsintered refractory layer can result from rapid electrical power ramp-up, dips in furnace temperature or operating the anode for too long between EAF campaigns. In extreme cases, the liquid steel may penetrate the bottom of the furnace when anode wear progresses too close to the bottom shell, which is extremely dangerous and must be avoided. The current state of the art for monitoring bottom anode wear employs thermocouples embedded in the anode pins at points in the anode. However, this approach is not sensitive enough to detect localized damage to the anode, especially when cracking occurs. The present work utilizes fiber-optic sensors to monitor the health of the anode by creating a real-time spatially distributed temperature map of the anode. Unlike traditional thermocouples, these sensors can be mounted at significantly greater depths, provide distributed temperature measurements, and can withstand temperatures of up to 900°C. Additionally, they are able to perform temperature measurements with a spatial resolution of 1.3 mm at a 5 Hz acquisition rate, providing unprecedented high-density real-time monitoring of anode health and increasing the efficiency, and safety of EAF operation.

## Introduction

Electric arc furnace (EAF) steelmaking accounts for approximately 70% of the steel production in the United States, characterized by utilizing electricity and recycled ferrous scrap, resulting in reduced carbon emissions.<sup>1</sup> Despite its energy efficiency ranging from 45 to 60%, there exists potential for further optimization. However, parameters necessary for optimization extend beyond the current monitoring capabilities. Effective operation

of EAFs relies significantly on the integrity and performance of critical components, particularly the bottom anode structure in DC EAFs.<sup>2</sup> Various designs of bottom anodes have been employed.<sup>3</sup> However, in this study, the focus is on a specific bottom anode design comprised of pins embedded within the refractory and connected to the EAF's power supply to facilitate the flow of electrical current from the electrode to the molten metal pool during steelmaking processes.<sup>4</sup>

Monitoring the condition of the bottom anode is essential as its wear and integrity directly impact the furnace's productivity and safety.<sup>2</sup>

Traditional approaches to assessing bottom anode health rely on single-point temperature measurements using thermocouples embedded within a subset of anode pins.<sup>2,5–8</sup> This method has limitations in providing comprehensive insights into the condition of the refractory material and the interface between the anode and the liquid steel pool. Moreover, this method necessitates reliance on predicted temperature profiles.<sup>9</sup> Bottom anode monitoring in EAFs is critical in completing the electrical circuit necessary for sustaining electric arcs within the furnace.<sup>10</sup> These arcs, generated between the bottom anode and the upper graphite electrode, are fundamental to the steelmaking process, making proper functioning of the bottom anode imperative for efficient operation.

In recent years, advancements in sensor technology, particularly the advent of fiber-optic sensors, have

opened new avenues for monitoring various components in steelmaking.<sup>11,12</sup> Unlike traditional thermocouples, fiber-optic sensors are miniature in size, offer real-time distributed temperature monitoring with immunity to electromagnetic interference (EMI), and are compatible with high-voltage, high-magnetic-field environments with seamless integration with control systems for scientific and industrial applications.<sup>13–17</sup> This presents an opportunity to overcome the limitations of conventional monitoring methods and provide more accurate and comprehensive insights into the condition of the bottom anode.

Fig. 1 illustrates the schematic representation of a conventional single-mode optical fiber, comprising a dielectric waveguide with a core made of germanium-doped silica, enclosed by a silica cladding. The outer layer consists of a polymer coating, usually composed of acrylate or polyimide, to enhance the mechanical durability of the optical fiber. This commercially accessible optical fiber is applicable as a distributed temperature sensor when coupled with Fiber Bragg Grating (FBG) technology.

Figure 1

Standard single-mode optical fiber for distributed temperature sensing.<sup>18</sup>

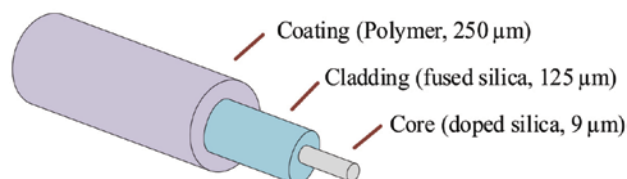
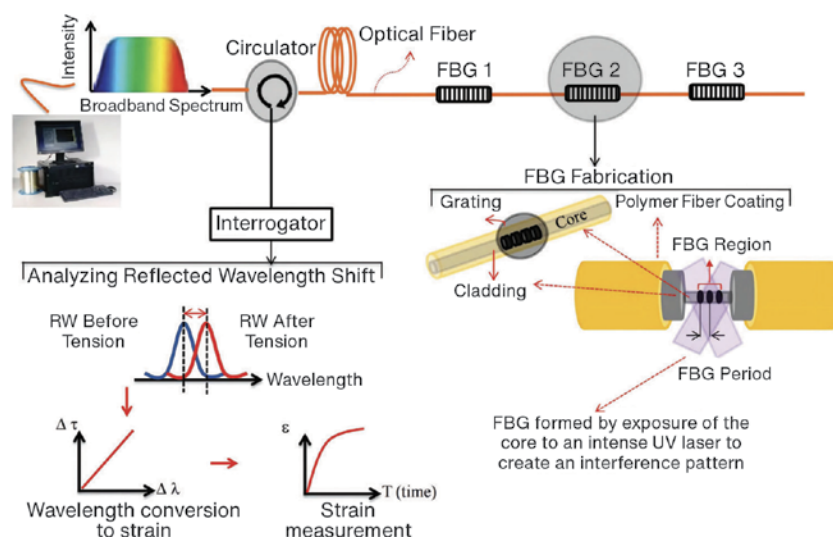


Figure 2

Fiber Bragg Grating (FBG) sensing technology.<sup>19</sup>



### Fiber Bragg Grating Sensing Technology

Fiber Bragg Grating sensing technology represents a potential advancement in temperature monitoring within industrial settings, offering increased precision and reliability. Utilizing the properties of optical fibers, FBG sensors consist of periodic etched structures — known as gratings — embedded within the fiber core. When exposed to temperature variations, such gratings undergo slight changes in periodicity, resulting in shifts in wavelength of reflected light along the fiber as depicted in Fig. 2. By precisely measuring these wavelength shifts, FBG sensors can accurately determine temperature changes with high resolution and sensitivity.

FBG sensors also exhibit immunity to electromagnetic interference and exceptional durability toward vibrations, making them ideal for harsh environments such as electric arc furnaces. This technology provides a new means for monitoring bottom anode wear, providing real-time temperature data essential for optimizing furnace performance, ensuring operational safety and maximizing productivity.

The expression for the Bragg wavelength ( $\lambda_B$ ) is given by:<sup>20</sup>

$$\lambda_B = 2n\Lambda \quad (\text{Eq. 1})$$

where  $n$  is the core's refractive index and  $\Lambda$  is the grating period.

For an input light source of operating wavelength  $\lambda$ , the corresponding change in  $\lambda_B$  due to change in temperature  $\Delta T$ , is expressed as:

$$\Delta\lambda_B = \lambda(\alpha\zeta)\Delta T \quad (\text{Eq. 2})$$

Here,  $\alpha$  is the coefficient of thermal expansion of the fiber and  $\zeta$  is the thermo-optic coefficient of the fiber.

The present work details the current progress attained by implementing fiber-optic-based temperature sensing on bottom anode pin of an industrial-scale EAF by leveraging FBG sensing technology. The efficacy of this measurement technique in capturing the temperature measurements on the anode pins shows promise for monitoring cyclic thermal load<sup>21</sup> on the anode pins and to determine the efficiency of the anode cooling systems. Several mathematical models<sup>4,21–23</sup> have been developed to study the temperature distributions in the EAF bottom anode. Since thermocouples are placed away from the induced current zone,<sup>23</sup> it is challenging to validate the temperature distributions from these models. But as fibers are immune to EMI, and it is possible to get measurements from these induced current zones, it would be valuable to determine the temperature distributions in the bottom anode.

## Methodology

### Laboratory Experiments

Experiments were conducted in the lab to assess the performance of the fiber-optic channel configuration, simulating conditions like those expected in a bottom anode pin in an industrial EAF environment. While complete replication of industrial bottom anode conditions is not feasible, a simulative testing approach was adopted.

### Test Apparatus

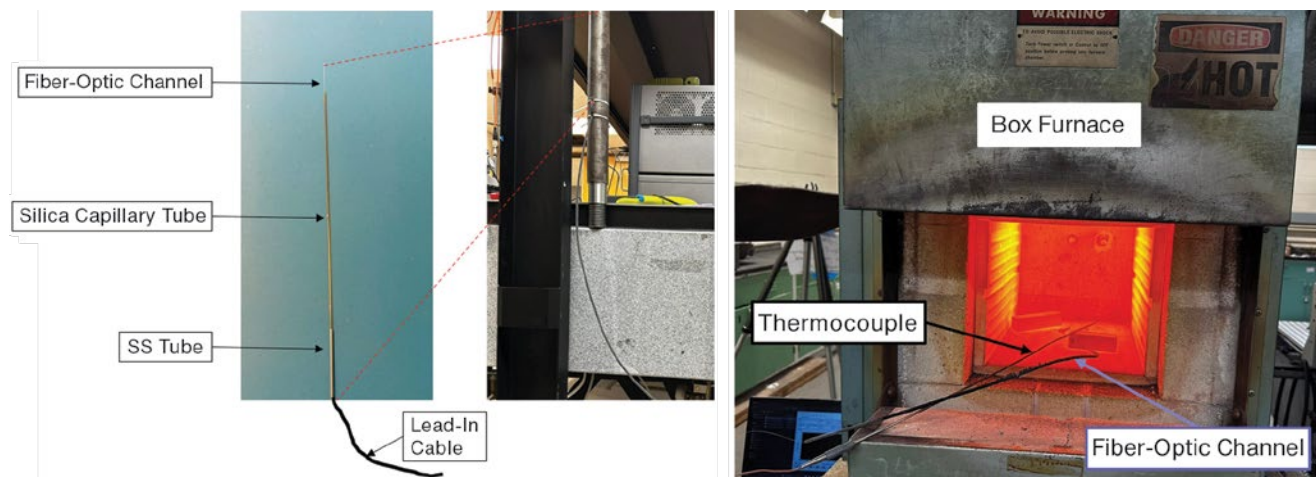
A box furnace served as the experimental setup for this study, providing a controlled environment conducive to evaluating the fiber-optic channel configuration's robustness and signal quality at high temperatures. The fiber-optic channel configuration was comprised of a polymer-coated single-mode fiber (SMF) housed within a fine silica capillary tube (inner diameter of 0.53 mm and wall thickness of 0.14 mm), which, in turn, was encased within a stainless steel (SS) tube with an inner diameter of 1.12 mm and wall thickness of 0.15 mm. To ensure safety, a fiberglass sleeve was utilized to join the silica capillary tube to the SS tube below the pin to create a break in the electrical circuit through the SS protecting tube to mitigate any potential shock hazards associated with electric leakage currents between the anode and the data collection system. A similar configuration was employed for plant trials.

### Test Procedure

Within the box furnace, the fiber-optic channel was securely positioned alongside a thermocouple for comparison. The furnace temperature was gradually increased to 900°C to test each component of the fiber-optic channel configuration for robustness and performance at elevated

Figure 3

Laboratory testing of the fiber-optic sensor configuration using box furnace.



temperatures. This experimental setup also allowed for assessment of signal quality when the optical fiber was subjected to different bending radii to simulate passage of the fiber through the furnace bottom plate, simulating potential bending scenarios encountered while instrumenting EAF anode pins in the plant.

### Plant Trials

After successful validation through laboratory testing, subsequent research involved application of this technology in plant trials. The objective was to validate and optimize deployment of fiber-optic sensors on a few outermost bottom anode pins that could be easily accessed for installation. All plant trials were conducted on a 150-ton DC EAF at Big River Steel – A U. S. Steel Co. in Osceola, Ark., USA. These trials were focused on demonstrating temperature measurements of the bottom anode and utilizing these measurements to calculate heat flow and cooling system efficiency through a full furnace campaign, thereby documenting the thermal profile of the EAF during different furnace operations. In this industrial implementation, single-mode optical fibers with FBG sensors were deployed. These sensors can accurately measure temperatures up to 900°C, but offer limited spatial resolution, typically capturing temperature data only at several predetermined locations along the length of fiber. However, FBGs provide uninterrupted temperature data even in extreme operating conditions.

To ensure accurate sensor placement, a fine 1.14-mm square groove was machined on the lower half of the anode pin, as shown in Fig. 4. This groove served as the

designated space for embedding an optical fiber housed within a fine silica capillary tube, which was then securely encased within a SS tube for added durability and protection. A refractory mortar was then applied to secure the embedded optical fiber, housed within a SS tube, in the groove on the anode pin. Within this fiber channel, three FBG sensors were fabricated at predetermined positions: FBG-1 was located 7 inches from the anode base, while FBG-2 and FBG-3 are positioned at heights of 5 inches and 3 inches, respectively. Additionally, each anode pin was also equipped with a thermocouple to continuously capture temperature measurements at 4 inches from the anode base. After instrumentation of the pins, the entire anode section was relocated to a maintenance stand to install the anode assembly into the furnace shell and pack it with refractory ramming mix. The shell was then transported to its operational position within the meltshop. Throughout the experimental period, anode temperature measurements were recorded every second from all three FBG sensors. The data collection was performed in two stages: (1) Initial data collection was performed over 10 days of operation, averaging 40 heats per day, providing a comprehensive data set; (2) Second data collection was planned at the end of EAF campaign, about 1,050 hours. However, only one hour of temperature measurement at the end of the campaign could be recorded due to an unrelated computer system failure.

Figure 4

Fiber-optic channel configuration and installation on the bottom anode pin of an electric arc furnace (EAF).

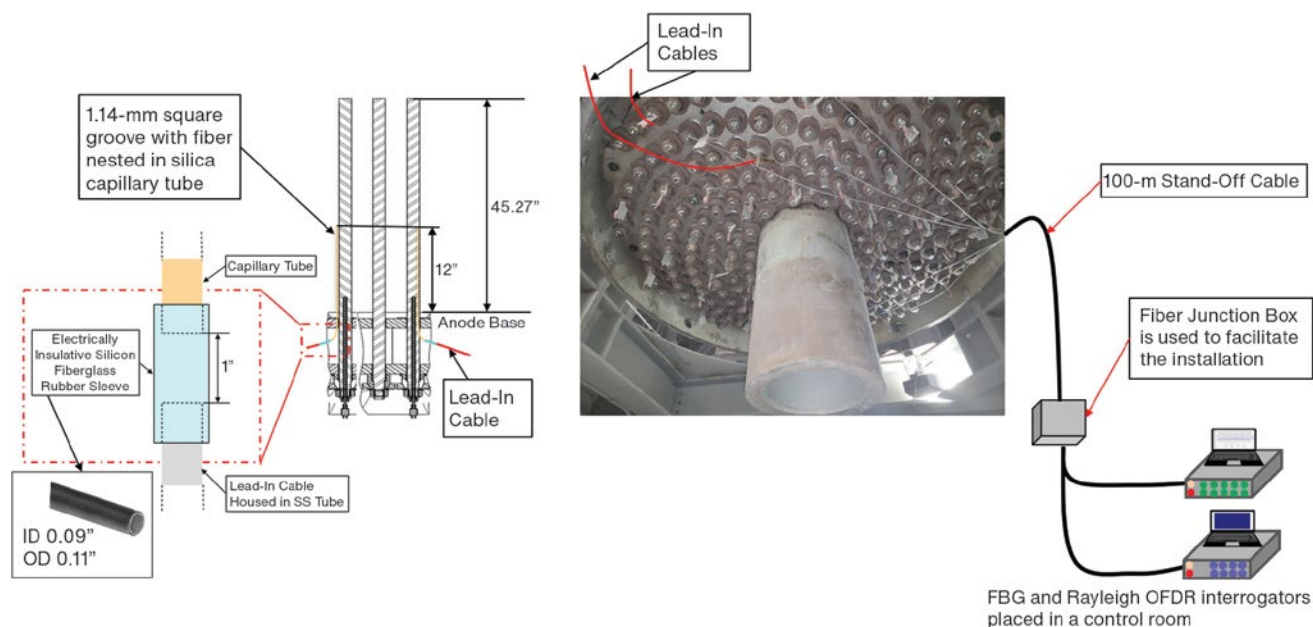




Figure 5

Stability test of the fiber-optic channel configuration with Fiber Bragg Grating (FBG) sensor.

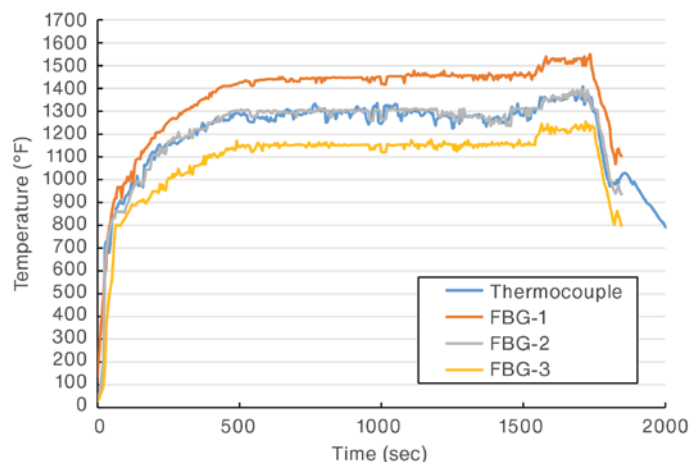
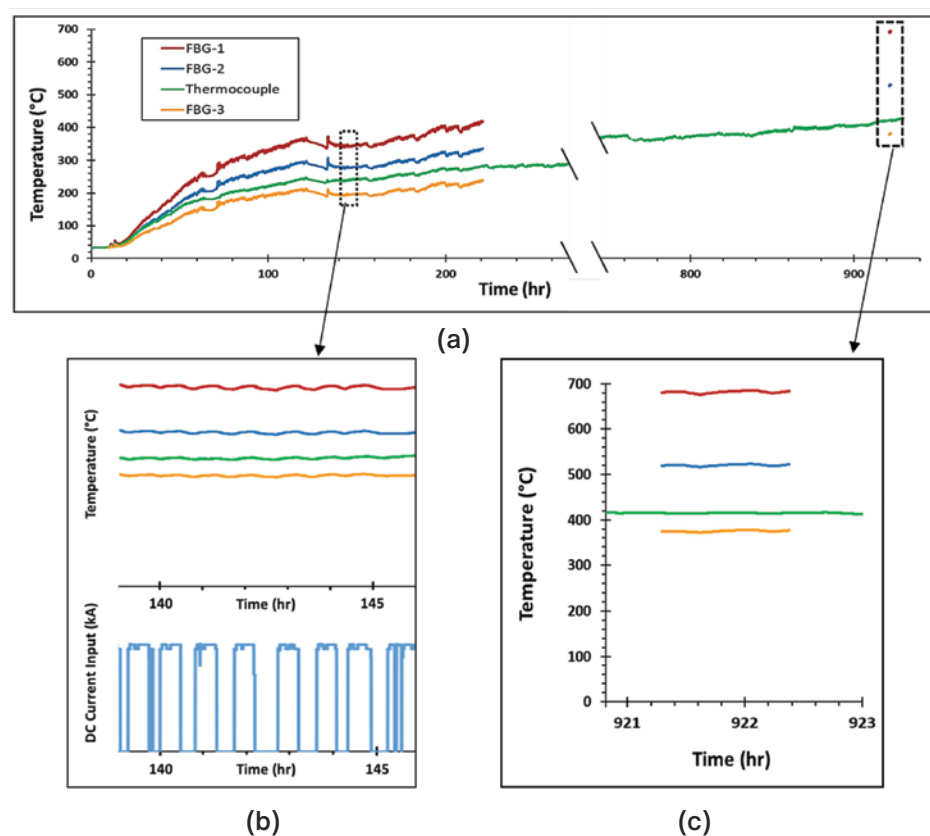


Figure 6

FBG temperature measurement data comparison with anode thermocouple data showing: 220 hours of FBG and thermocouple data (a), temperature fluctuation correlation with furnace DC current (b), and 1.5 hours of data at the end of EAF campaign (c).



## Results and Discussion

The laboratory testing of the fiber-optic sensor that simulated industrial conditions demonstrated the functionality of temperature measurement and fiber sheathing configuration. Fig. 5 shows a smooth temperature profile recorded by the FBG sensor during these tests. To balance the signal robustness and installation convenience, a maximum temperature of 800°C and an optimal bending angle of 45° for the lead-in cable extending from the pin and out of EAF anode section was selected for subsequent use in industrial trials. The stability test depicted in Fig. 5 demonstrated the reliability of the fiber-optic channel configuration for subsequent temperature measurements from the anode pins of an industrial EAF.

Plant trials were conducted on the 150-ton DC EAF at Big River Steel – A U. S. Steel Co. The fiber sheathing design proved effective in protecting the fiber from damage and strain during

the ramming of the bottom anode refractory. Moreover, the relocation of the instrumented anode section, along with a 30-m-long lead-in cable to the maintenance stand, followed by the furnace shell transfer to the operating position with the meltshop, was performed successfully without damaging the optical fiber.

Using a 1 Hz data acquisition rate and a fiber channel fabricated with three FBG sensors positioned at different predetermined heights, the initial data collection process spanned over 10 days, averaging 40 heats per day, providing a comprehensive data set for subsequent analysis. Following 38.5 days of continuous operation and several scheduled maintenance events, a second data collection process was initiated to validate the durability of the fiber-optic sensors near the end of the EAF campaign, spanning approximately

1,050 hours. In Fig. 6a, data from one of the instrumented pins equipped with three FBG sensors is presented. Additionally, Fig. 6b illustrates the correlation between the temperature fluctuations observed in the temperature measurements of the FBG sensors and the thermocouple data, aligning with variations in furnace electrical energy inputs and operating cycles. Fig. 6c shows a magnified view of the highlighted area from Fig. 6a, affirming that the optical fiber survived the harsh conditions of EAF steelmaking processes for an entire furnace campaign.

## Conclusions

Demonstration of fiber-optic sensors for monitoring the bottom anode of an EAF shows promise for advancing the efficiency and safety of steelmaking processes. The plant trials conducted at Big River Steel – A U. S. Steel Co. demonstrated successful deployment and effective operation of fiber-optic sensors on an operational EAF. Notably, installation and mounting of the fiber in an anode pin survived ramming of the furnace bottom, transport and installation of the furnace, and in-service operation for a full furnace campaign, demonstrating the feasibility of this technology. Granularity of temperature measurements and correlation with furnace power input indicates that fiber-optic instrumentation may also be used to assess furnace operating conditions. Further

research and applications could lead to enhanced process control, increased operational efficiency and elevated safety protocols in electric arc furnace steelmaking processes.

## Future Work

The temperature data provided by fiber-optic sensors will be utilized in future work to calculate the total heat flux through the bottom anode. This data will enable more accurate estimates of the temperature distribution along the anode pins and within the adjacent refractory layer to track and predict bottom wear during operation. With these measurements, a deeper understanding of dynamic thermal conditions within the furnace, leading to improved refractory wear and improved operational performance can be achieved.

## Acknowledgment

This work is supported by the U.S. Department of Energy's Office of Energy Efficiency and Renewable Energy (EERE) under the Advanced Manufacturing Office Award Number DE-EE0009392. The views expressed herein do not necessarily represent the views of the U.S. Department of Energy or the United States government.

*This article is available online at AIST.org for 30 days following publication.*

## References

1. American Iron and Steel Institute, Sustainable Steelmaking, AISI 11, 2021.
2. Kaplun, M.Y., "Bottom Electrodes of DC Electric Arc Furnaces," *Russian Metallurgy (Metally)*, 2009, pp. 618–621.
3. *ibid.*
4. Timoshenko, S., and Gubinskij, M., "Energy Efficient Solutions of DC Electric Arc Furnace Bottom Electrode," *Modern Problems of Metallurgy*, 2020, pp. 121–129, doi:10.34185/1991-7848.2020.01.12.
5. Azbukin, V.D., and Malinovskii, V.S., "Device for Controlling the State of a Bottom Electrode," USSR Inventor's Certificate No. 438368.
6. Shelepov, N.S., "Bottom Electrode for Melting Furnaces," U.S. Patent 4101725.
7. Kaltenbach, M.J., "Sensor System for Bottom Electrodes of an Electric Arc Furnace," U.S. Patent 0072011 A1, 2014.
8. Al-Nasser, M. et al., "Effect of Compressibility on Industrial DC Electric Arcs," *Results in Engineering*, Vol. 19, 2023.
9. Heberlein, J.; Mentel, J.; and Pfender, E., "The Anode Region of Electric Arcs: A Survey," *Journal of Physics D: Applied Physics*, Vol. 43, 2010 <https://doi.org/10.1088/0022-3727/43/2/023001>.
10. Szekeley, J.; McKelliget, J.; and Choudhary, M., "Heat-Transfer Fluid Flow and Bath Circulation in Electric-Arc Furnaces and DC Plasma Furnaces," *Ironmaking and Steelmaking*, Vol. 10, 1983, pp. 169–179.
11. Zhang, B. et al., "In Situ and Real-Time Mold Flux Analysis Using a High-Temperature Fiber-Optic Raman Sensor for Steel Manufacturing Applications," *Journal of Lightwave Technology*, Vol. 41, 2023, pp. 4419–4429.
12. Spierings, T.; Kamperman, A.; Hengeveld, H.; Kromhout, J.; and Dekker, E., "Development and Application of Fiber Bragg Gratings for Slab Casting," *AISTech 2017 Conference Proceedings*, 2017, pp. 8–11.
13. Roman, M. et al., "A Spatially Distributed Fiber-Optic Temperature Sensor for Applications in the Steel Industry," *Sensors*, Vol. 20, 2020, p. 3900.
14. Brusa, E.; Delprete, C.; and Giorio, L., "Smart Manufacturing in Rolling Process Based on Thermal Safety Monitoring by Fiber Optics Sensors Equipping Mill Bearings," *Applied Sciences*, Vol. 12, 2022, p. 4186.
15. Inalegwu, O.C.; Gerald II, R.E.; and Huang, J., "A Machine Learning Specklegram Wavemeter (MaSWave) Based on a Short Section of Multimode Fiber as the Dispersive Element," *Sensors*, Vol. 23, 2023, p. 4574.
16. Alla, D.R. et al., "Cascaded Sapphire Fiber Bragg Gratings Inscribed by Femtosecond Laser for Molten Steel Studies," *IEEE Trans Instrum Meas*, Vol. 73, 2024, pp. 1–8.
17. Snider, E.B.; Kumer Saha, R.; Dominguez, C.; Huang, J.; and Bristow, D.A., "Embedding Fiber-Optic Sensors in Metal Components via Direct Energy Deposition," *Solid Freeform Fabrication Symposium – An Additive Manufacturing*, 2023.



TOLL FREE (855) 4BECKER  
GWBCRANE.COM

**MORE  
THAN  
JUST  
CRANES**

INSPECTIONS

ENGINEERING

BELOW-THE-HOOK DEVICES

FIELD SERVICE REPAIRS

AUTOMATION

REPAIR PARTS

TRAINING

**AISTech  
Booth  
1200**

## Technical Article

18. Roman, M. et al., "Peritectic Behavior Detection in the Fe-C-Mn-Al-Si Steel System Using Fiber Optic Temperature Mapping," *AISTech 2020 Conference Proceedings*, 2020, pp. 822-833.
19. Qu, J. et al., "Recent Progress in Advanced Tactile Sensing Technologies for Soft Grippers," *Advanced Functional Materials*, Vol. 33, 2023, <https://doi.org/10.1002/adfm.202306249>.
20. Othonos, A., "Fiber Bragg Gratings," *Review of Scientific Instruments*, Vol. 68, 1997, pp. 4309-4341.
21. Moro, L.; Benasciutti, D.; and De Bona, F., "Simplified Numerical Approach for the Thermo-Mechanical Analysis of Steelmaking Components Under Cyclic Loading: An Anode for Electric Arc Furnace," *Ironmaking and Steelmaking*, Vol. 46, 2019, pp. 56-65.
22. Hay, T.; Visuri, V.V.; Aula, M.; and Echterhof, T., "A Review of Mathematical Process Models for the Electric Arc Furnace Process," *Steel Research International*, Vol. 92, 2021, <https://doi.org/10.1002/srin.202000395>.
23. Zhut, P.; Lowke, J.J.; Morrow, R.; and Haidat, J., "Prediction of Anode Temperatures of Free Burning Arcs," *J. Phys. D: Appl. Phys.*, Vol. 28, <http://iopscience.iop.org/0022-3727/28/7/014>. ♦



This paper was presented at AISTech 2024 — The Iron & Steel Technology Conference and Exposition, Columbus, Ohio, USA, and published in the AISTech 2024 Conference Proceedings.

